Magnetic and Electronic Transport Properties of $CaMn_{1-x}Nb_xO_3$

Yongquan Guo* and Wei Li

Division of Functional Materials, Central Iron & Steel Research Institute, 76 Xueyuan Nanlu Street, Beijing 100081, China

Sujoy Roy and Naushad Ali

Department of Physics, Southern Illinois University, Carbondale, Illinois 62901-4401

Received February 7, 2005. Revised Manuscript Received March 19, 2005

Polycrystalline $CaMn_{1-x}Nb_xO_3$ compounds ($x = 0.1, 0.2, 0.3$) were synthesized by a solid reaction. $CaMn_{1-x}Nb_xO_3$ crystallizes in an orthorhombic $GdFeO_3$-type structure. The Nd doping causes the increases of the lattice parameters, unit cell volume, the average Mn−O bond distance, and Mn−O−Mn bond angle. $CaMn_{1-x}Nb_xO_3$ compounds show magnetic phase inhomogeneity. With increasing the Nb concentration, $CaMn_{1-x}Nb_xO_3$ compounds exhibit ferromagnetic, metamagnetic, antiferromagnetic, and paramagnetic characterizations, respectively. And their magnetizations significantly reduce. $CaMn_{1-x}Nb_xO_3$ compounds are insulators in the temperature range from 5 to 400 K, and their resistivities enhance with increasing Nb content. A huge asymmetry resistivity hysteresis loop is observed for the $CaMn_{0.9}Nb_{0.1}O_3$ compound at low temperature; however, this resistivity loop is melting with increasing the applied field and temperature and tends to disappear near the Curie temperature. This phenomenon might be due to the Nb doping inducing a low-temperature magneto-electric phase separation between the ferromagnetic metallic and the charge-ordering antiferromagnetic insulating phases.

Introduction

Since a huge decrease of the resistivity in the expitaxially grown $La_{2/3}Ca_{1/3}MnO_3$ film was found by Jin et al.,[1] a renewed interest has grown in the study of the electronic transport and the magnetic properties as well as the colossal magnetoresistance (CMR) effect of the alkaline-earth doped manganese oxides with ABO_3 perovskite structure in recent years.[2,3] The double-exchange mechanism proposed by Zener,[4] the Jahn−Teller(JT) polarization,[5] and the tolerance factor[6] have been used to interpret the colossal magnetoresistance effect in these manganite perovskites. More recently, the fascinating physics of the CMR materials has been driven by the close coupling between the lattice, the electronic, and magnetic degrees of freedom, which has generally shown the electronic phase separation between the different magneto-electronic states at low temperature.[7,8] According to the double exchange-mechanism, the ferromagnetic exchange interaction, which involves the e_g hopping electrons, can be controlled by the Mn^{4+}/Mn^{3+}. The ratio between the Mn^{4+} and Mn^{3+} ions can be controlled by the substitution of the element with a higher valence number than Mn^{3+} at the Mn crystal position. An attempt has been made to carry out this designation by a pentavalent Nb or Ta ions substitution for Mn ions in calcium manganite.[9,10] A larger magnetoresistance effect was observed at low temperature.[9] However, the field dependence of resistivity characterization and its change with the temperature were not investigated yet, and the Jahn−Teller effect was not mentioned in the previous studies either. These studies on the lattice-electron and the magnetic-electron couplings are beneficial for understanding the special electronic transport characteristics associated with the lattice distortion and magnetic phase transition in $CaMn_{1-x}Nb_xO_3$ compound. In this paper, we studied the correlation between the lattice, electronic, and magnetic phases, as well as the related electron transport property in $CaMn_{1-x}Nb_xO_3$ compound.

Experimental Procedure

Polycrystalline $CaMn_{1-x}Nb_xO_3$ ($x = 0.1,0.2,0.3$) was synthesized by a solid-state reaction. Stoichiometeric amounts of Nb_2O_5, MnO_2, and $CaCO_3$ powders were thoroughly mixed and calcined at 1373 K for 48 h. The mixture was ground, pelletized, and sintered at 1523 K for 72 h. The crystal structure was determined by a Rigaku automatic X-ray diffractometer and was refined by the Rietveld's method.[11] The thermo-magnetic property was measured by a

* To whom correspondence should be addressed.

(1) Jin, S.; Tiefel, T. H.; McCormack, M.; Fastnacht, P. A.; Ramesh, R.; Chen, L. H. *Science* **1994**, *264*, 413.
(2) Xiong, G. C.; Li, Q.; Ju, H. L.; Mao, S. N.; Sanapati, L.; Xi, X. X.; Greene, R. L.; Venkatesam, T. *Appl. Phys. Lett.* **1995**, *66*, 1427.
(3) Guo, Y. Q.; Liu, Y. C.; Tao, K.; Zhuo, H. P.; Wappling, R. *J. Solid State Chem.* **1999**, *148*, 236.
(4) Zener, C. *Phys. Rev.* **1951**, *82*, 403.
(5) Millis, A. J.; Littlewood, P. B.; Shraiman, B. I. *Phys. Rev. Lett.* **1995**, *74*, 5144.
(6) Hwang, H. Y.; Cheong, S.-W.; Radaelli, P. G.; Marezio, M.; Batlogg, B. *Phys. Rev. Lett.* **1995**, *75*, 914.
(7) Adams, C. P.; Lynn, J. W.; Mukovaski, Y. M.; Aresenov, A. A.; Shulyatev, D. A. *Phys. Rev. Lett.* **2000**, *85*, 3954.
(8) Deac, I. G.; Mitichell, J. F.; Schiffer, P. *Phys. Rev. B* **2001**, *63*, 172408.
(9) Raveau, B.; Zhao, Y. M.; Martin, C. et al., *J. Solid State Chem.* **2000**, *149*, 203.
(10) Xu, G. J.; Funahashi, R.; Pu, Q. et al. *Solid State Ion.* **2004**, *171*, 147.
(11) Rietveld, H. M. *J. Appl. Crystallogr.* **1969**, *2*, 65.

10.1021/cm050289p CCC: $30.25
Published on Web 04/21/2005

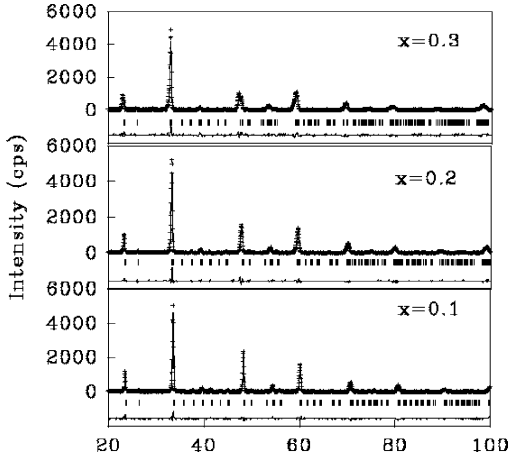

Figure 1. Refined XRD patterns of the $CaMn_{1-x}Nb_xO_3$, where the experimental and the calculated XRD patterns are marked by the "+" point and the solid line, respectively. The lowest trace indicates the difference between the two patterns. The peak positions of the orthorhombic structures are denoted by the middle vertical lines.

Table 1. Refined Lattice Parameters and Unit Cell Volumes of $CaMn_{1-x}Nb_xO_3$ Compounds

Nb content x	$x = 0.1$	$x = 0.2$	$x = 0.3$
a (Å)	5.306(3)	5.348(0)	5.444(0)
b (Å)	5.330(5)	5.385(1)	5.389(6)
c (Å)	7.513(3)	7.556(2)	7.585(6)
cell volume (Å^3)	212.5(2)	217.6(2)	222.5(6)

commercial SQUID magnetometer from 4 to 400 K at an applied field of 0.1 T. Both the zero-field-cooling (ZFC) and the field-cooling (FC) processes were performed during the magnetization measurement. The temperature dependence of magnetoresistance was measured by a standard four-probe technique from 4 to 400 K at a zero field and an applied field of 5 T, respectively. The applied field dependencies of magnetoresistance and magnetization measurements were carried out in fields ranging from −5 to 5 T and temperatures ranging from 5 to 120 K.

Results and Discussion

Structure and Distortion of the MnO_6 Octahedron. Powder XRD patterns show that the single phase with an orthogonally distorted perovskite structure is obtained in $CaMn_{1-x}Nb_xO_3$ samples. The experimental and the refined XRD patterns of $CaMn_{1-x}Nb_xO_3$ compounds have been shown in Figure 1. Both the lattice parameters and the unit cell volumes increase with increasing the Nb content, as listed in Table 1, which agrees with the previous report.[10] This phenomenon can be interpreted by the average ionic size at the Mn position. On one hand, since the radius of the Nb pentavalence ion (0.78 Å) is larger than that of the Mn^{4+} ion (0.67 Å), thus the substitution of the Nb^{5+} ion for the Mn^{4+} ion causes the increase of the average radius at the Mn position and induces the lattice expansion. On the other hand, according to charge balance law, the partial substitution of the Nb^{5+} ions for the Mn^{4+} ions will cause the presence of the Mn^{3+} ions in the $CaMn_{1-x}Nb_xO_3$ compound. And the radius of the Mn^{3+} (0.72 Å) ion is also larger than that of the Mn^{4+}(0.67 Å); thus, the presence of Mn^{3+} ions also increases the average radius at the Mn position. The ionic occupations and refined R factors (R_p and R_{wp}) as well as good fit factors (s) of the $CaMn_{1-x}Nb_xO_3$ compounds are listed in Table 2. In each unit cell, there are four kinds of

Table 2. Ionic Occupations and Refined R Factors (R_p and R_{wp}) as Well as Good Fit Factors(s) of $CaMn_{1-x}Nb_xO_3$ Compounds

(Mn^{3+}, Mn^{4+}, Nb^{5+}): 4a (0,0,0)				
Nb content x		$x = 0.1$	$x = 0.2$	$x = 0.3$
Ca^{2+}:	4c (1)	x, 0.4872(4)	0.4797(9)	0.4686(2)
	(x, y, $^1/_4$)	y, 0.0358(8)	0.0378(7)	0.03104(6)
$O^{2-}{}_I$:	4c(2)	x, 0.5729(3)	0.5640(6)	0.5076(6)
	(x, y, $^1/_4$)	y, 0.4797(1)	0.4815(3)	0.4775(6)
$O^{2-}{}_{II}$:	8d	x, 0.1982(1)	0.1980(8)	0.2058(7)
	(x, y, z)	y, 0.3017(5)	0.2934(7)	0.3104(6)
		z, 0.0327(9)	0.0264(3)	0.0369(8)
R_p		8.1%	9.3%	10.7%
R_{wp}		11.0%	12.5%	14.2%
s		1.3	1.4	1.6

Table 3. Calculations of the MnO_6 Octahedron Distortions (Average Mn−O Bond Distance, Mn−O−Mn Bond Angle, and Coordination Numbers) and the Tolerance Factors of $CaMn_{1-x}Nb_xO_3$ Compounds

Nb content x	$x = 0.1$	$x = 0.2$	$x = 0.3$
<Mn−O> (Å)	1.931	1.935	1.951
N	6	6	6
<Mn−O−Mn>	153.59°	156.48°	158.31°
N	6	6	6
tolerance factor	0.926	0.932	0.943

equivalent crystal positions, i.e., the 4a, 4c(1), 4c(2), and 8d, which are occupied by 4 (Mn^{3+}, Mn^{4+}, Nb^{5+}), 4 Ca^{2+}, 4 $O^{2-}{}_I$, and 8 $O^{2-}{}_{II}$, respectively.

The Jahn−Teller polarization is derived from the distortion of the MnO_6 octahedron, which can change the e_g charge density of the Mn ion. The electronic ground state of the Mn^{3+} ion is degenerated and its energy is lowered by a spontaneous distortion of the surrounding lattice. In our experiment, the Jahn−Teller effect has been investigated by calculating the (Mn,Nb)−O bond distances and (Mn,Nb)−O−(Mn,Nb) bond angles according to the refined ionic occupation parameters. The Nb doping results in the increases of the (Mn,Nb)−O bond distances and the (Mn,Nb)−O−(Mn,Nb) bond angles. According to the electron−lattice interaction model proposed by Millis,[12] the tolerance factor can affect the electrons hopping process by adjusting the static crystal structure, which involves the conventionally dynamical electron−phonon coupling; it can link the instantaneous deviation of atoms from their ideal crystallographic position to the instantaneous deviation of electron configuration from the average value. In our case, the tolerance factor has been calculated according to the equation[6]

$$t = \frac{d_{A-O}}{\sqrt{2}d_{Mn-O}}$$

The tolerance factor enhances with increasing the Nb concentration. The calculations of the MnO_6 octahedron distortions and tolerance factors are listed in Table 3.

Magnetic and Electronic Transport Properties. $CaMn_{1-x}Nb_xO_3$ compounds exhibit very complicated inhomogeneous magnetic phases as shown in Figure 2. $CaMn_{0.9}Nb_{0.1}O_3$ compound shows a spin glass state at 45.86 K in FC and ZFC measurements as shown in the inset in Figure 2, and then a charge ordering antiferromagnetic phase at 124.2 K,

(12) Millis, A. J. *Nature* **1998**, *392*, 147.

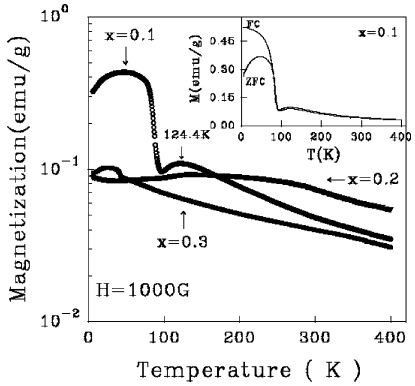

Figure 2. Temperature dependence of magnetization of $CaMn_{1-x}Nb_xO_3$. The inset shows the FC and ZFC measurements of $CaMn_{0.9}Nb_{0.1}MnO_3$.

and a paramagnetic−faramagnetic transition at 90.2 K, respectively. With increasing the Nb concentration, $CaMn_{1-x}Nb_xO_3$ compounds correspond to show a low-temperature metamagnetic phase and a weak ferromagnetic order for $x = 0.2$ and a low-temperature antiferromagnetic order-like magnetic phase for $x = 0.3$. The origin ferromagnetic order in $CaMn_{1-x}Nb_xO_3$ compound comes from the double-exchange (DE) interaction between the Mn^{3+} and the Mn^{4+} ions. Since the Nb^{5+} doping causes the presence of Mn^{3+} ion. The Mn^{3+} ion provides the electron source for the hopping e_g electron, and the Mn^{4+} ion makes a hole for carrying the e_g electron. The DE interaction occurs in the $Mn^{3+}-O-Mn^{4+}$ pair. The DE interaction requires the e_g electrons to have the same spin orientation during hopping in the $Mn^{3+}-O-Mn^{4+}$ pair; therefore, the exchanging interaction between these e_g electrons forms the ferromagnetic order. However, the high content of Nb in the $CaMn_{1-x}Nb_xO_3$ compound can cause two issues. The one is the lattice expansion due to the increase of the average size at the Mn site, and the other one is the reduction of magnetizations due to the nonmagnetic Nb ion substitution for the magnetic Mn ion. These issues affect the magnetic properties of $CaMn_{1-x}Nb_xO_3$ compound. On one hand, the ferromagnetic DE interaction is related to the Mn−O bond distance and $Mn^{3+}-O-Mn^{4+}$ bond angle. If the Mn−O bond distance increases, the separation between the magnetic ions increases and it induces weakening of the ferromagnetic order. In our experiment, since the high content of Nb in the compound causes the prolongation of the average (Mn,-Nb)−O bond distance and the increase of the $Mn^{3+}-O-Mn^{4+}$ bond angle, such a Jahn−Teller effect suppresses the DE ferromagnetic interaction; thus, the DE ferromagnetic interaction is significantly weakened and induces a significant decrease of the magnetization of the $CaMn_{1-x}Nb_xO_3$ compound. On the other hand, the concentration of the electron carrier gradually reduces with increasing the Nb content in $CaMn_{1-x}Nb_xO_3$ compound, which is due to the reduction of Mn^{4+} ion content. This causes the possible presence of the antiferromagnetic $Mn^{3+}-O-Mn^{3+}$ pair in $CaMn_{1-x}Nb_xO_3$ compound. In this case, the antiferromagnetic $Mn^{3+}-O-Mn^{3+}$ pair coexists with the ferromagnetic $Mn^{3+}-O-Mn^{4+}$ pair in the compound. The competition between the two interactions affects directly the magnetic property of the $CaMn_{1-x}Nb_xO_3$ compound. The magnetic characterization might depend on the ratio between the antiferromagnetic

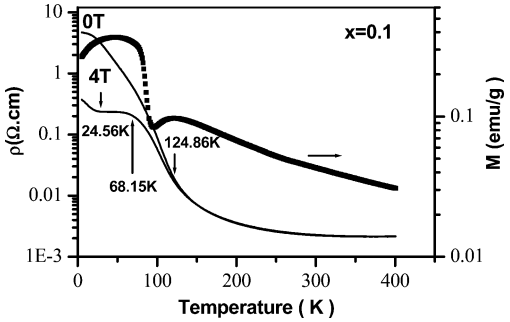

Figure 3. Temperature dependence of magnetoresistance and magnetization of $CaMn_{0.9}Nb_{0.1}MnO_3$.

$Mn^{3+}-O-Mn^{3+}$ pair and the ferromagnetic $Mn^{3+}-O-Mn^{4+}$ pair in $CaMn_{1-x}Nb_xO_3$ compound. Thus, the magnetic properties of $CaMn_{1-x}Nb_xO_3$ compounds show the ferromagnetic, the metamagnetic, and the paramagnetic phases with increasing Nb concentration. Reference 9 reported the effect of a small amount of Nb doping on the magnetic properties of the $CaMn_{1-x}Nb_xO_3$ with $x = 0-0.10$; the $CaMn_{1-x}Nb_xO_3$ compounds showed the ferromagnetic order in the Nb concentration range from 0.02 to 0.06. The magnetic inhomogeneous phenomenon was also observed in the sample with $x = 0.1$. However, the difference between the magnetization of the ferromagnetic phase and the charge ordering peak was very small. In our case, this difference is much larger. This phenomenon might depend on the applied fields and measurement process such as FC and ZFC. In our measurement, both FC and ZFC measurements were carried out at an applied field of 0.1 T; however, the ZFC measurement was only performed at a higher field (1.45 T) in ref 9. Reference 10 only reported the electronic transport of $CaMn_{1-x}Nb_xO_3$ with $x = 0.1-0.3$ at high temperature, but the magnetic and electronic transport properties at low temperature were not investigated.

$CaMn_{1-x}Nb_xO_3$ compound exhibits the insulating characteristics in the temperature range from 5 to 400 K at a zero field. And the resistivity obviously increases in Nd high region; it might be due to the decrease of the electronic carrier concentration with increasing the Nb content. However, a field-induced insulator−metal (IM) transition is observed in the $CaMn_{0.9}Nb_{0.1}O_3$ compound at an applied field of 4 T. This special transport phenomenon was not observed in ref 9. In their study, no electric phase transformation occurred in this compound; the $CaMn_{0.9}Nb_{0.1}O_3$ compound showed insulating characteristics before and after applying a magnetic field of 7 T. The resistivity reduced greatly at low temperature by applying a high magnetic field of 7 T. They called this phenomenon a "low temperature huge magnetoresistance effect". However, the field dependence of the resistivity and its change with the temperature were not investigated in their study either. The reason they missed observing the field-induced electric phase transition in the $CaMn_{0.9}Nb_{0.1}O_3$ compound might be due to the higher field they applied or the characterization of their samples. The transport property was not investigated in the temperature change from 5 to 400 K in ref 10.

Electron-Magnetic Interaction and MR Effect. Figure 3 shows the temperature dependence of resistivity and magnetization of $Ca_{0.9}Nb_{0.1}MnO_3$ compound. It shows the

relationship between the electric and magnetic phases. An electronic phase transformation is associated with a magnetic transition. The field-induced insulator−metal transition associated with a low-temperature spin glass such as antiferromagnetic state occurs at 24.56 K. While a MI transition associated with a ferromagnetic−paramagnetic transition is observed at 68.15 K, the antiferromagnetic charge ordering state occurs at the crossing point of the two resistivity−temperature curves measured at a zero field and an applied field of 4 T, respectively. The low-temperature insulator−metal transition can be interpreted as the applied field driving the antiferromagnetic insulating state to the ferromagnetic metallic state. The magnetic field-induced IM transition has been found in the previous studies of the $Nd_{1/2}Sr_{1/2}MnO_3$ and the $Pr_{1-x}Ca_xMnO_3$ crystals.[13,14] This phenomenon was initially interpreted by the change of the magnetization in which the resistivity showed a magneto-electronic phase transition from the antiferromagnetic insulating state to the ferromagnetic metallic state, which is caused by the application of an external magnetic field. From the thermodynamic point of view, both of the states are almost energetically degenerate, but the free energy of the ferromagnetic state decreases by the Zeeman energy $-M_sH$ (M_s is the spontaneous magnetization) so that the magnetic field-induced transition would occur by applying an external magnetic field of a few Tesla. It destabilizes the antiferromagnetic state and drives the phase transition to the ferromagnetic metallic state; therefore, these two phases coexist at low temperature. With increasing applied magnetic field, the content of the ferromagnetic metallic phase enhances, and the concentration of the antiferromagnetic insulating phase reduces. More recently, the above-mentioned two-phase phenomenon has generally been taken as an electronic phase separation between different magnetoelectronic states at low temperature.[7] 10% Nb doping in $CaMnO_3$ induces a huge asymmetrical field-dependent resistivity hysteresis loop at low temperature as illustrated in Figure 4. However, this loop is melting with increasing the field and the temperature and tends to disappear near T_C temperature. The formation of the huge asymmetrical resistivity hysteresis loop might be due to the field driving the antiferromagnetic moment alignment rotating in the direction of the applied field gradually, and induces a magneto-electric phase transformation from the antiferromagnetic insulating phase to the ferromagnetic metallic phase. Therefore, the electron scattering effect in the antiferromagnetic phase tends to be obviously suppressed with increasing the applied field. It involves a significant debilitation of the electron scattering interaction for the antiferromagnetic insulating phase and induces a huge decrease of the resistivity. This dramatic change of the field-dependent resistivity causes the formation of a huge asymmetrical resistivity hysteresis loop in this compound. This special phenomenon was also observed in our previous study on the electronic transport of the $Yb_xCa_{1-x}MnO_3$ compound.[15] If the spin-dependent electron

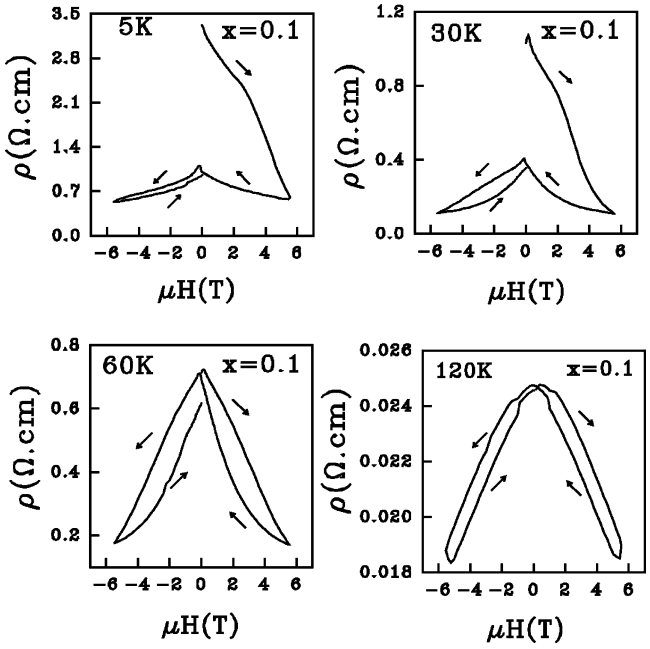

Figure 4. Applied field dependence of magnetoresistance of $CaMn_{0.9}Nb_{0.1}MnO_3$.

scattering at the magnetic domain boundaries is totally responsible for the observed magnetoresistance (MR), then the MR magnitude is scaled by the square of the spin-polarization of the carriers, namely, $(M/M_s)^2$ (where M_s is the saturation magnetization).[16] But this correlation between the MR and the spin-polarization does not fit our experimental data. It reveals that the special electronic transport characterization does not come from the magnetic domain. However, the MR ratio is obviously associated with the magnetization since the field dependence of magnetization curves shows the same asymmetric loop as that observed in the resistivity loop in fields ranging from −5 to 5 T at 5 K as shown in Figure 5, where the magnetization saturation could not be achieved at a maximum applied field of 5 T. The asymmetric resistivity loop starts to melt and tends to be symmetric near the Curie temperature with increasing temperature.

The field-dependent resistivity and magnetization measurement were carried out at 5 K for three cycles. However, the results are identical. It implies that the direction of the applied magnetic field also affects the magnetization and the resistivity characteristics at low temperature. In this study, the effect on resistivity of the application of the positive magnetic is obvious; the resistivity is significantly reduced with application of the positive magnetic field, which might be caused by a magneto-electric phase transformation from the antiferromagnetic insulating phase to the ferromagnetic metallic phase driven by a positive field. However, the resistivity is not reversible by decreasing the applying field, not even by applying a negative field. This implies that the antiferromagnetic insulating state cannot be recovered no matter how much the applied field decreases even with a negative field. This phenomenon can be understood by a phase separation between the antiferromagnetic insulating phase and the ferromagnetic metallic phase. The antiferro-

(13) Schiffer, P.; Ramirez, A. P.; Bao, W.; Cheong, S. W. *Phys. Rev. Lett.* **1995**, *75*, 3336.
(14) Tomioka, Y.; Asamitus, A.; Moritomo, Y.; Kokutra, Y. *J. Phys. Soc. Jpn.* **1995**, *65*, 3626.
(15) Guo, Y. Q.; Roy, S.; Ali, N. *J. Appl. Phys.* **2002**, *91*, 7394.
(16) Xiao, J. Q.; Jiang, J. S.; Chien, C. L. *Phys. Rev. Lett.* **1992**, *68*, 3749.

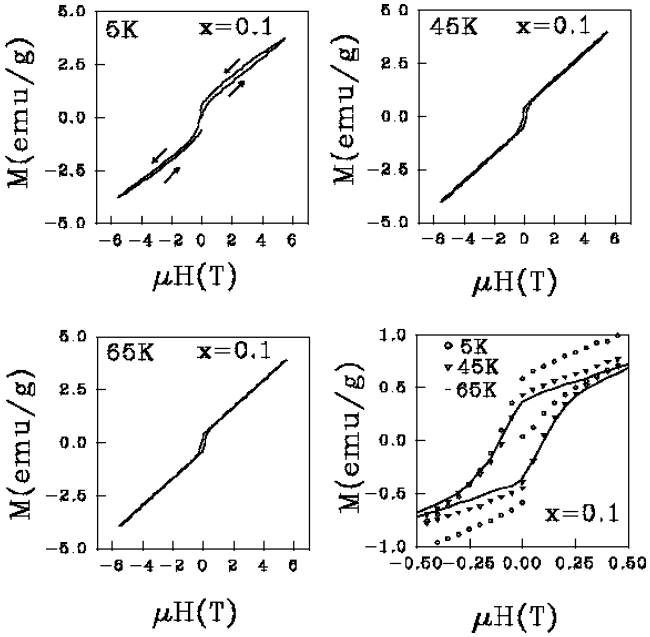

Figure 5. Applied field dependence of magnetization of $CaMn_{0.9}Nb_{0.1}MnO_3$.

magnetic insulating phase has already been suppressed by the initial application of the positive field and becomes unstable in this case; therefore, the applied field drives a magneto-electronic phase transition from the antiferromagnetic insulating phase to the canting ferromagnetic metallic phase or the ferromagnetic metallic phase.

The spin glass-ferromagnetic transition occurs at 45.86 K. When the temperature increases more than this transition temperature, the spin glass insulating states disappears and induces a decrease of the resisitivity. The resistivity loop is melting with increasing the temperature, and its asymmetric resistivity loop also is gradually adjusted to be symmetrical with increasing temperature. This phenomenon can be understood by the temperature-dependent insulator characterization. Since $CaMn_{1-x}Nb_xO_3$ compound exhibits insulating characteristics in the temperature range from 5 to 400 K, its resistivity reduces with increasing temperature. So the difference between the resistivities before and after applying a field tends to decrease with increasing temperature. Therefore, the resistivity loop exhibits a melting behavior with increasing temperature.

Conclusion

In conclusion, $CaMn_{1-x}Nb_xO_3$ crystallizes in an orthogonally distorted perovskite structure. Both the lattice parameters and unit cell volumes increase with increasing Nb content. Nb doping induces the increase of the average Mn−O bond length and Mn−O−Mn bond angle. $CaMn_{1-x}Nb_xO_3$ compounds exhibit very complicated magnetic and electric inhomogeneous phases. A magnetic field induced insulator−metal transition is found in $CaMn_{0.9}Nb_{0.1}O_3$ compound. The huge asymmetric magnetization hysteresis and resistivity loops are observed at low temperature, which might be interpreted by an electro-magnetic phase separation between the spin glass antiferromagnetic insulating state and the ferromagnetic metallic state or the field-induced canting ferromagnetic metallic state.

Acknowledgment. This work is supported by CARS-University of Chicago.

CM050289P